

High-Throughput ^{19}F NMR Chiral Analysis for Screening and Directed Evolution of Imine Reductases

Shucheng Song,^{II} Chenyang Wang,^{II} Wenjing Bao, Zhenchuang Xu, Jian Wu, Liang Lin,* and Yanchuan Zhao*



Cite This: ACS Cent. Sci. 2025, 11, 1094–1102



Read Online

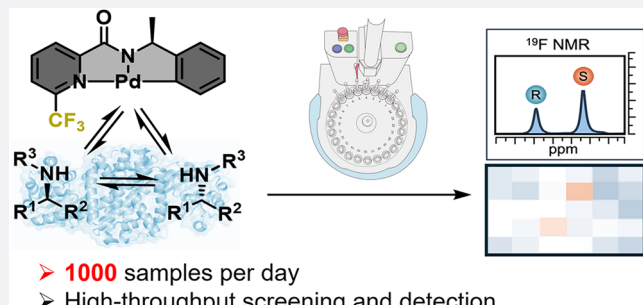
ACCESS |

Metrics & More

Article Recommendations

Supporting Information

ABSTRACT: Biocatalysis is an essential tool for asymmetric synthesis, significantly enhancing the production of chiral molecules. As advancements in protein screening and engineering rapidly evolve, the demand for efficient, rapid chiral analysis methods has intensified. Addressing this need, we introduce a high-throughput ^{19}F NMR-based assay that provides comprehensive insights into the enantioselectivity, stereopreference, and yields of biocatalytic reactions. This assay has been successfully applied to screen imine reductases, showcasing its efficacy in the directed evolution for synthesizing an intermediate of the anti-Parkinson drug, rotigotine. Our method offers substantial promise for propelling forward the fields of biocatalysis and synthetic biology by accelerating the assessment of stereochemical outcomes in biocatalytic processes.



- 1000 samples per day
- High-throughput screening and detection
- Simultaneous determination of ee and yield

INTRODUCTION

Biocatalysis has emerged as an essential technique across diverse fields, including organic synthesis and pharmaceutical development, valued for its mild reaction conditions, exceptional selectivity—encompassing enantio-, chemo-, and regioselectivity—and its environmental advantages.^{1–6} This approach is particularly effective in asymmetric synthesis of carbon–carbon and carbon–heteroatom bonds. For instance, terpene cyclases efficiently transform unsaturated terpene backbones into cyclic terpenoids with impressive stereoselectivity.⁷ Diels–Alderases facilitate the asymmetric [4 + 2] cyclizations that form cyclohexane rings prevalent in natural products.^{8–11} Moreover, enzymes like cytochrome P450 and iron- α -ketoglutarate-dependent oxygenases (Fe/ α KGs) are gaining recognition for their ability to introduce oxygen into unreactive C–H bonds.^{12–17} The field of biocatalysis is rapidly advancing with the integration of directed evolution, which is further bolstered by the use of machine learning and automated processes in reaction setup and workup. Innovations in high-throughput screening technologies have dramatically accelerated enzyme screening, offering rapid, efficient evaluations and shifting away from the traditionally slow pace of enzyme analysis to enhance screening capacity.¹⁸ Despite these advances, challenges remain in precise chiral screening, where dependence on traditional chiral high-performance liquid chromatography (HPLC) analysis considerably limits the efficiency of the iterative “design-build-test” loop in asymmetric biocatalysis.^{19–25}

To enhance the enantioanalysis of biocatalytic reactions, various strategies have been employed. A prominent approach is the use of isotopically labeled pseudoenantiomers or pseudo-meso-compounds, as demonstrated by Reetz and colleagues.²⁶ This method measures enantioselectivity by comparing the ratio of nonlabeled to labeled products, which can be conveniently determined using techniques such as nuclear magnetic resonance (NMR), and mass spectrometry (Figure 1A).^{26,27} Alternatively, enantioselectivity can be assessed by comparing reaction rates between enantiopure and racemic substrates, with monitoring through changes in fluorescence or heat generation.^{28,29} These methods are effective for screening various kinetic resolutions and desymmetrization reactions (Figure 1A), although they are generally not suitable for reactions involving prochiral substrates. Recently, Kroutil and colleagues have developed an ingenious approach for screening peroxygenases in C–H oxidations, utilizing the formation of nicotinamide adenine dinucleotide phosphate (NADPH) from the highly enantioselective dehydrogenase-catalyzed oxidation of the secondary alcohol product. This serves as a probe for the enantioselectivity of the C–H oxidation (Figure 1B).³⁰

Received: March 18, 2025

Revised: May 20, 2025

Accepted: May 21, 2025

Published: June 3, 2025



ACS Publications

© 2025 The Authors. Published by
American Chemical Society

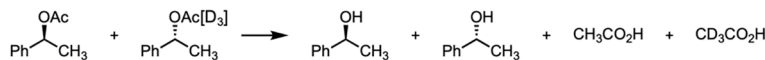
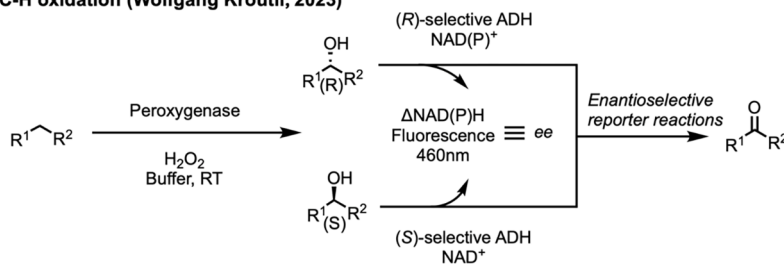
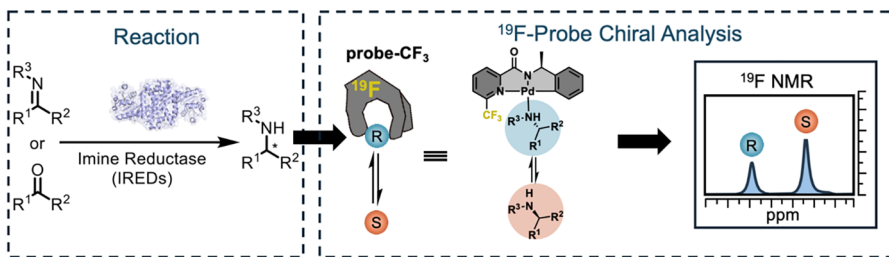
A. Kinetic resolution (Manfred T. Reetz, 1999)**B. C-H oxidation (Wolfgang Kroutil, 2023)****C. Imine reduction—This work**

Figure 1. High-throughput chiral detection methods for biocatalysis. (A) Chiral analysis of biocatalytic kinetic resolution enabled by isotope labeling. (B) Fluorescence-based method for chiral analysis of biocatalytic C–H oxidation. (C) ¹⁹F NMR-based method for chiral analysis of biocatalytic imine reduction.

Additional sophisticated methods include the use of circular dichroism (CD), which leverages reversible interactions and covalent derivatization of target chiral analytes to induce significant Cotton effects and characteristic CD signals.^{31–34} Despite significant advancements, there remains a significant need for rapid screening methods for amines, which are indispensable in the synthesis of natural products and in pharmaceutical development. Addressing this, the development of specialized enantioanalysis techniques for imine reductases and reductive aminases is crucial. In this regard, we have introduced a novel ¹⁹F NMR-based assay for rapid screening of biocatalytic reactions producing chiral amines. With NMR spectrometer equipped with a regular autosampler, this method could assess enantioselectivity, stereopreference, and reactivity approximate 1000 samples per day (Figure 1C). By employing this assay in directed evolution experiments, we enhanced the enantioselectivity of a reductive amination reaction to produce an intermediate of the anti-Parkinson drug from 40% enantiomeric excess (ee) to 99%, illustrating its potential to refine biocatalytic methods efficiently.

RESULTS AND DISCUSSION

The rapid enantioanalysis of amines from biocatalytic reactions presents significant challenges. One primary issue is the use of NADPH or its analogs in imine reduction reactions, which absorb ultraviolet (UV) light strongly and can interfere with UV or fluorescence-based detection methods. Such interference often leads to inaccurate correlations between the optical signal and the enantiocomposition. Additionally, the use of cell lysates instead of purified enzymes in biosynthetic screening introduces variability due to their undefined composition, which can cause further interferences. Another major hurdle is the development of rapid chiral analysis methods that are effective for both primary and secondary amines. Secondary

amines, in particular, pose a greater challenge due to their increased steric bulkiness,^{35–37} even though they are the desired products in many biocatalytic imine reduction and reductive amination reactions and are prevalent in natural products and critical pharmaceuticals. Moreover, the detection of chiral substances in biocatalytic systems is complicated by low concentrations of chiral products and the presence of substrates, enzymes, and byproducts, which create a complex matrix obscuring detection. This increases the difficulty of accurately detecting and quantifying chiral substances. However, current methods, including fluorescence and CD, often rely on changes in optical signal intensity and do not provide discrete signals for each enantiomer, undermining detection fidelity in complex samples and requiring relatively controlled conditions. To address these challenges, we propose the use of a suitable ¹⁹F-labeled probe in conjunction with ¹⁹F NMR, which could provide a viable solution for rapid chiral screening in biocatalytic reactions. A probe that reversibly binds chiral analytes eliminates the need for covalent derivatization, allowing immediate detection upon mixing with the target sample (Figure 1C).^{38–40} The distinct advantages of ¹⁹F NMR, including high sensitivity and low background noise, provide robust anti-interference capabilities, facilitating rapid detection and quantification of minimal analyte quantities.^{41–43}

Establishment of the Enantioanalysis Platform. To evaluate the viability of our approach, we employed 5-methyl-3,4-dihydro-2H-pyrrole (**1**) as a model substrate (Figure 2). Upon reduction, it yields 2-methylpyrrolidine (**1a**) featuring a chiral carbon center connected to the nitrogen atom. Traditional chiral detection of 2-methylpyrrolidine via chromatography is hindered by its weak UV absorption, typically necessitating covalent derivatization followed by chromatographic separation. This process significantly impedes

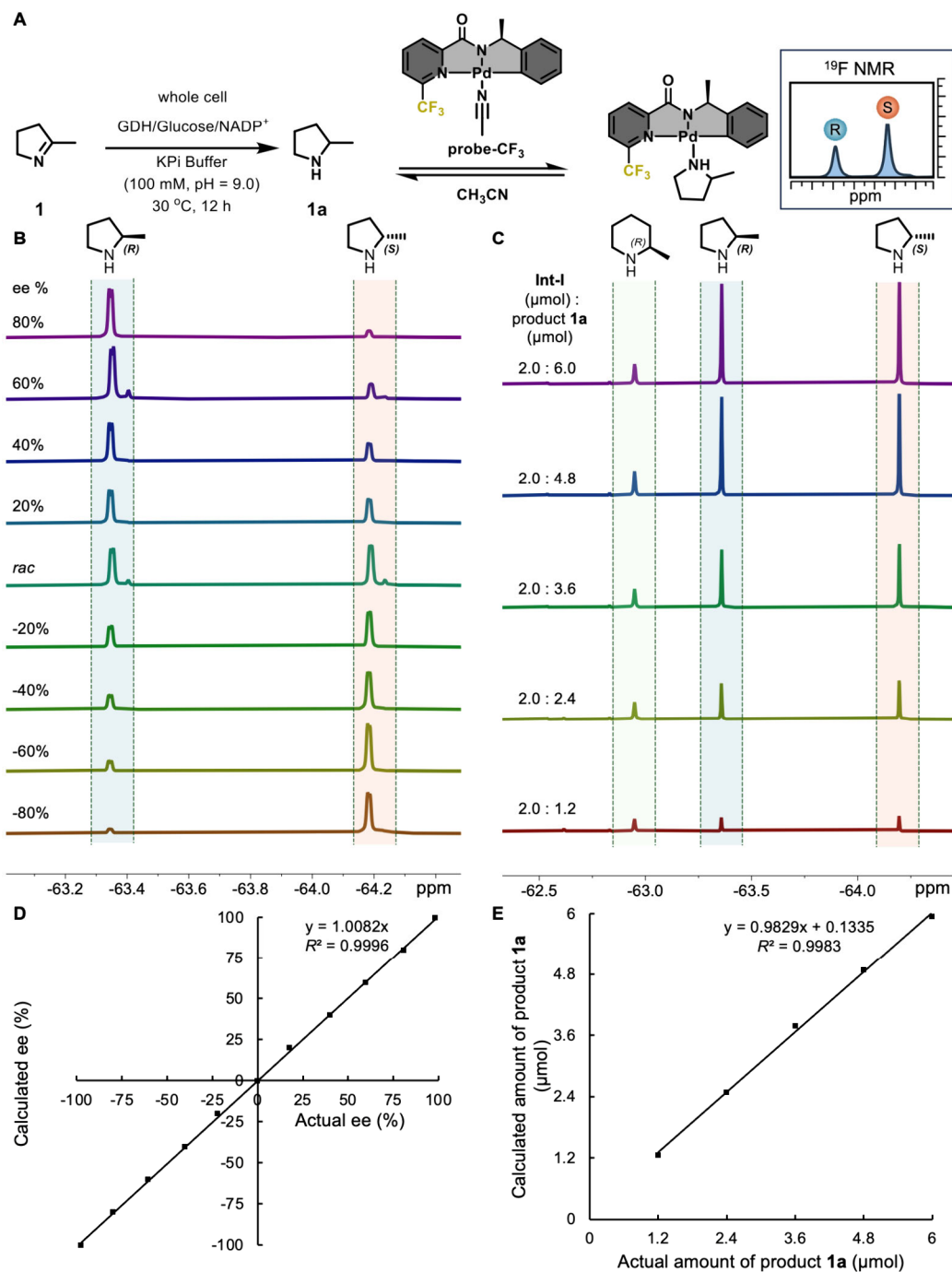


Figure 2. Determination of the ee values and yield using **probe-CF₃**. (A) Schematic representation of the imine reduction reaction and ¹⁹F NMR-based detection methodology. (B) ¹H-decoupled ¹⁹F NMR spectra (16 scans each) of a mixture of **probe-CF₃** (ca. 9 μmol) in CDCl₃ and 2-methylpyrrolidine (ca. 6 μmol) of varying enantiocompositions. (C) ¹H-decoupled ¹⁹F NMR spectra (16 scans each) of a mixture of **probe-CF₃** (ca. 9 μmol) in CDCl₃ and varying amounts of 2-methylpyrrolidine (ranging from 0 to 6 μmol) and 2 μmol of (R)-2-methylpiperidine (**Int-I**) as an internal standard. (D) Calibration plot showing the linear relationship between the measured and actual ee values. (E) Calibration plot depicting the linear correlation between the measured and actual amounts of 2-methylpyrrolidine.

the efficiency of biocatalytic reaction screenings. For the enantioanalysis of 2-methylpyrrolidine, we utilized a chiral ¹⁹F-labeled cyclopalladium probe (Figure 2A, **probe-CF₃**) characterized by its open binding site, which is essential for accommodating sterically bulky analytes and enhancing the recognition of complex secondary amines.⁴⁴ During detection, the probe interacts with various amine products and the substrate **1**, producing distinct ¹⁹F NMR signals for each species (Figures 2A–C and Figures S1,3,6 in SI). The

enantiomeric composition is accurately reflected in the integrals of these signals. To address the slight variations in the probe's binding affinity toward the R and S enantiomers of **1a**, we introduced a correction coefficient to adjust for biases in ee determination arising from differential complexation. This correction factor is readily calculated from the ratio of the integrals of ¹⁹F NMR signals obtained from the analysis of racemic samples (Figure S2 in SI).³⁷ Our investigation has demonstrated that this method can precisely evaluate the

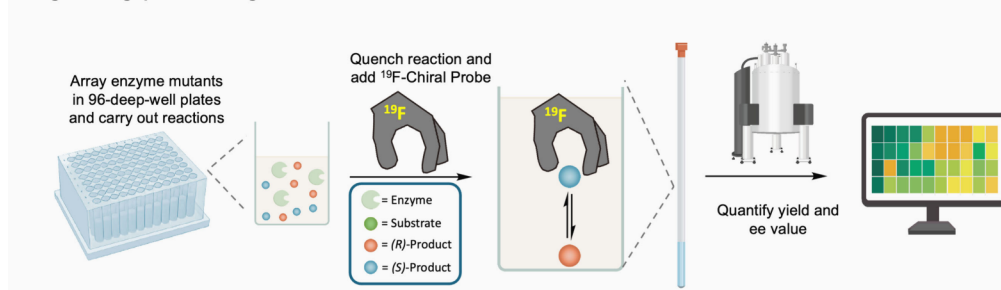
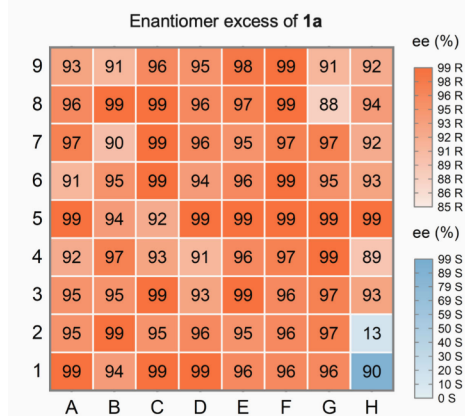
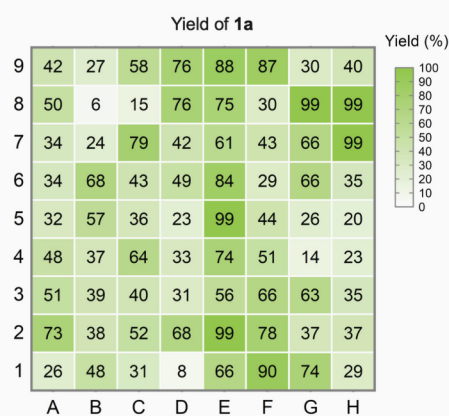
A. High-throughput screening flowchart**B. High-throughput screening result of ee****C. High-throughput screening result of yield**

Figure 3. (A) Schematic workflow of the high-throughput NMR chiral screening process. (B) Enantioselectivities of the screened biocatalytic reactions, determined by ^{19}F NMR analysis. (C) Yields of the screened biocatalytic reactions, quantified by ^{19}F NMR relative to an internal standard. Reaction conditions: 300 μL reaction volume, substrate **1** (20 mM), NADP^+ (0.5 mM), BmGDH (1 mg/mL), D-glucose (30 mM), KPi buffer (100 mM, pH 9.0), 800 rpm, 30 °C, 12 h. The product yield was quantified by ^{19}F NMR analysis relative to an internal standard. The enantiomeric excess (ee) values were determined using ^{19}F NMR.

enantiocomposition of the target sample, showing an excellent linear correlation between the measured ee values and the actual enantiocomposition (Figure 2D). Notably, this technique typically exhibits a deviation of less than 2%,^{39,44} offering significantly greater accuracy compared to other separation-free enantioanalysis methods. Moreover, the capability of directly detecting the *R* and *S* enantiomers of the amine product enhances the fidelity of the detection process, facilitating the easy identification of impurities or byproducts. This feature is crucial for screening biocatalytic reactions and is difficult to achieve with alternative methods. Evaluating the conversion of biocatalytic reactions is crucial for assessing enzyme performance. While various methods exist to determine the yield of biocatalytic transformations, the simultaneous determination of both yield and enantioselectivity is particularly valuable, as it provides comprehensive information and prevents the oversight of crucial details that might occur if either efficiency or selectivity is screened in isolation. Accurate yield determination using chiral dynamic ^{19}F NMR probes has long been challenging, as incomplete binding between the probe and the analyte can lead to significant errors when relying on direct integration of the ^{19}F NMR signals. To address this limitation and facilitate the quantification of conversion, (*R*)-2-methylpiperidine (**Int-I**) was introduced as an internal standard (Figure 2C and Figure S3 in SI). This compound competes with the target product for the binding site of **probe-CF₃**. By comparing the relative integrals of the ^{19}F signals of the internal standard to those of the product enantiomers, both conversion and enantioselec-

tivity can be simultaneously determined (Figures 2D, 2E and Figures S1 to S5 in SI). This method enhances the accuracy and comprehensiveness of our enzyme screening process, allowing for a more effective evaluation of biocatalytic reactions.

Screening of Imine Reductases. Having established methods to determine both conversion and enantioselectivity, we next applied this approach to the high-throughput screening of imine reductases for the reduction of specific substrates. Initially, we employed 12 of well-characterized enzymes^{45–56} as query sequences to conduct the basic local alignment search tool (BLAST) search against the non-redundant protein database hosted by the national center for biotechnology information (NCBI). Based on sequence similarity, we compiled a panel of 134 imine reductases (IREDs) (Table S11 in SI). These IREDs were then systematically tested to identify those that exhibited the desired catalytic activity and enantioselectivity. Following the enzymatic reactions (carried out in 96-well plates), the reaction mixture was combined with a deuterated chloroform solution containing **probe-CF₃** and an internal standard (**Int-I**). After thorough mixing and centrifugation, the deuterated chloroform phase was directly subjected to ^{19}F NMR analysis without further purification (Figure 3A). This process allows for the simultaneous evaluation of both yield and enantioselectivity based on the newly generated ^{19}F NMR signals (Figure 2). Due to the high sensitivity of this method, only 6 μmol of substrate is required for the analysis, aligning well with standard biocatalytic screening setups. The platform is highly

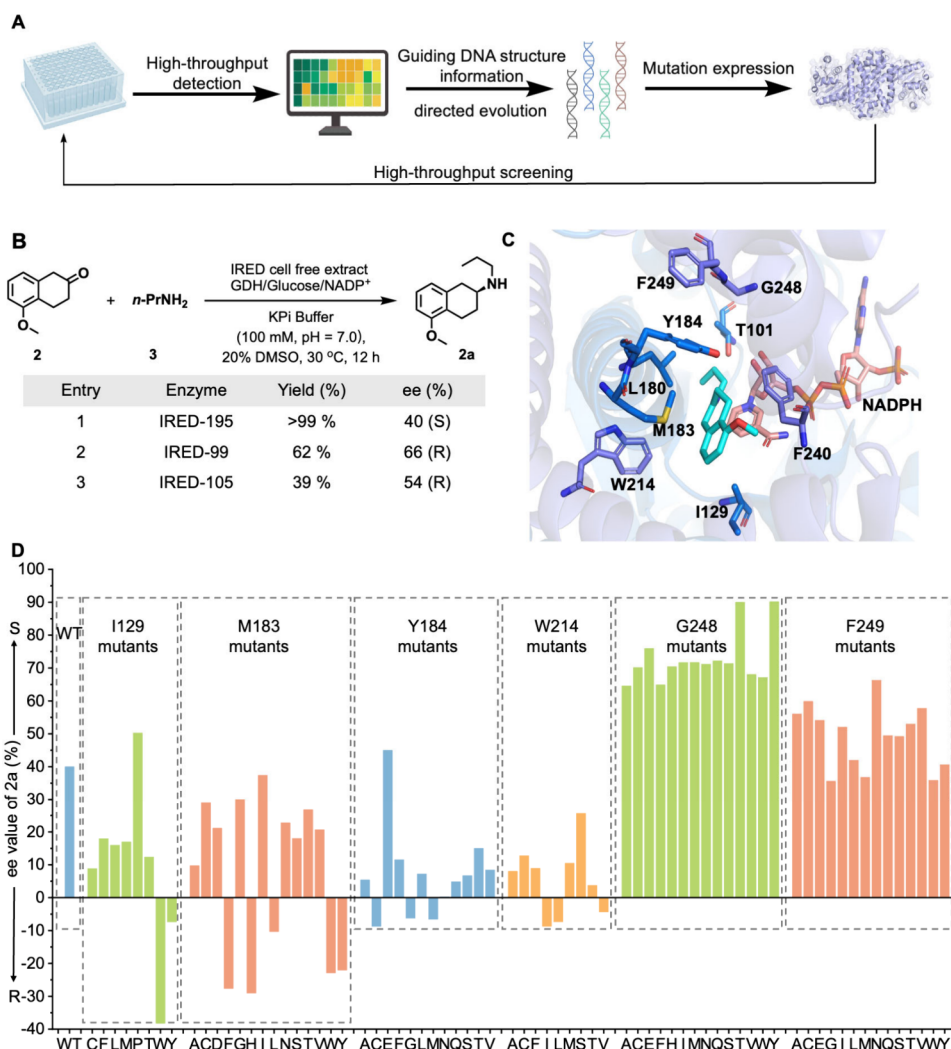


Figure 4. (A) Workflow of the directed evolution process. (B) Reaction scheme for the reductive amination reaction and enzyme screening results. Reaction conditions: 500 μ L reaction volume, cell-free extract 200 μ L, substrate **2** (10 mM), *n*-propylamine (1 M), NADP⁺ (0.5 mM), BmGDH (1 mg/mL), D-glucose (30 mM, 3 equiv), KPi buffer (100 mM, pH 7.0), DMSO (20%, v/v), 800 rpm, 30 °C, 12 h. The product yield was quantified by ¹⁹F NMR analysis relative to an internal standard. The enantiomeric excess (ee) values were determined using ¹⁹F NMR. (C) Molecular docking of the intermediate of the reductive amination of substrates **2** and **3** into the active cavity of IRED-195. (D) Enantioselectivity of IRED-195 (wild-type, WT) and its mutants at residue positions 129, 183, 184, 214, 248, and 249.

efficient, taking less than 1.5 min to determine both conversion and enantioselectivity for each reaction (Table S6 in SI). With an NMR spectrometer equipped with a standard autosampler, 24 samples can be analyzed in 35 min, requiring no further optimization of the spectroscopy or acceleration of the autosampling process. This setup allows for the screening of approximately 1,000 samples in a single day. Chromatographic resolution of chiral analytes typically takes 10 to 40 min per sample and often necessitates covalent derivatization for amine analysis (Figure S20). Our approach boosts analytical efficiency by at least 10 to 20 times, offering substantial potential to advance biosynthetic techniques. During the screening process, our platform swiftly identified that out of 134 IREDs, 79 demonstrated activity in reducing the substrate **1** to **1a**, exhibiting moderate to high activity levels (Figure 3C and Table S1 in SI). These enzymes showed considerable stereoselectivity, with the majority favoring the production of (*R*)-2-methylpyrrolidine. Notably, only three enzymes—IRED-186, IRED-191, and IRED-192—exhibited S-stereo-selectivity (Figure 3B and Table S1 in SI). Among these,

IRED-191 was particularly notable for its high S-selectivity, achieving an ee of 90% (S) (Table S1 in SI). To elucidate the molecular basis of stereoselectivity in imine reduction, we conducted a multiple sequence alignment of IREDs with R-selectivity and those with S-selectivity obtained through screening (Figure S18 in SI), and performed homology modeling on IRED-191. We then compared the simulated structure of IRED-191 with the known structures of R-selective IREDs (Figure S19 in SI).^{47,51,55} Our analysis revealed significant divergence at the catalytic residue. Aspartic acid (Asp) is consistently conserved in the active sites of R-selective IREDs. In contrast, the equivalent position in S-selective enzymes is predominantly occupied by either tyrosine (Tyr) or asparagine (Asn). This variation suggests a pivotal role in controlling enantioselectivity. This correlation between the identity of the catalytic residue and the enzyme's stereoselectivity underscores the significance of this position in defining both the catalytic mechanism and the stereochemical outcome. We further validated these findings using chiral HPLC. The ee values of 2-methylpyrrolidine **1a** produced by

IRED-181, IRED-185, and IRED-188, determined via chiral HPLC (which required derivatization and a 40 min chromatographic separation), were consistent with those measured by our ¹⁹F NMR platform. The deviation between the two methods was less than 1% (Figure S20–S24 and Table S5 in the SI), demonstrating the accuracy and reliability of our ¹⁹F NMR approach. Notably, our method is fully compatible with whole-cell-based enzymatic assays, as demonstrated by experiments showing that the ee values of products generated by IRED-191-expressing whole cells and corresponding cell lysates differed by less than 1% (Table S7 in SI). This analytical platform is not limited to analyzing 2-methylpyrrolidine **1a**; it can easily be adapted for the detection of other amines and N-heterocycles (Figures S12 – S17 and Table S4 in SI). For instance, when screening 1-methyl-3,4-dihydroisoquinoline, we identified 109 IREDS capable of facilitating its reductive transformation, which suggests a broader enzyme applicability for this substrate compared to substrate **1a**. Most enzymes still preferred *R*-selectivity, but nine enzymes (IRED-33, IRED-42, IRED-44, IRED-45, IRED-181, IRED-182, IRED-186, IRED-191, and IRED-192) exhibited *S*-selectivity. Remarkably, all *S*-selective enzymes except IRED-186 displayed excellent *S*-selectivity, with ee values exceeding 99% (Table S4 in SI). The findings underscore the versatility and efficiency of our NMR-based platform in rapidly screening a wide array of biocatalysts for both activity and selectivity across different substrates, highlighting its utility in accelerating the development of efficient, selective biocatalysts.

Directed Evolution of Imine Reductases. After establishing our screening platform and validating its performance across various template substrates, we next sought to demonstrate its broader application by conducting directed evolution targeting high-value compounds, including pharmaceutical intermediates (Figure 4A). Imine reductases are powerful biocatalysts for the asymmetric synthesis of optically pure amines, and recent advances have further underscored their strong potential for industrial application.^{48,57–59} To showcase the utility of our platform, we selected a key precursor to the anti-Parkinson drug rotigotine as a model target. The ability of wild-type enzymes to produce this intermediate with high enantioselectivity was previously demonstrated by Turner and co-workers in 2021.⁶⁰ Given the increasing importance of directed evolution and the necessity to screen large libraries of variants efficiently, this case study serves to validate the effectiveness of our ¹⁹F NMR-based screening platform and provides a route for accessing highly selective enzymes. The chiral amine component of rotigotine is in the *S*-configuration, prompting us to screen our IRED panel for this specific reaction (Figure 4B). It is noteworthy that propylamine, when used in excess, may compete with product **2a** for the binding site on probe-CF₃. Consequently, the residual propylamine was removed under reduced pressure after the reaction to minimize interference. In our investigation, IRED-105, IRED-99, and IRED-195 all exhibited substantial activity; however, only IRED-195 showed the desired *S*-selectivity. It achieved a high yield coupled with moderate enantioselectivity of 40% ee (Table S2 in SI). These results are consistent with those reported in previous studies.⁶¹ We then initiated directed evolution on IRED-195 by docking the imine intermediate into the enzyme's active site (Figure 4C). Docking studies identified nine amino acids within 4 Å of the substrate that potentially interact directly with it: T101, I129, L180, M183, Y184, W214, F240, G248, and F249. We

applied saturation mutagenesis to these residues and conducted high-throughput screening using our established NMR platform to assess both activity and stereoselectivity. From screening 171 mutants, the variants G248T and G248Y demonstrated significant improvements in enantioselectivity, increasing from 40% (*S*) in the wild type to 90% (*S*), while maintaining the original activity levels (Figure 4D and Table S3 in SI). Mutating I129 to a more rigid proline notably enhanced *S*-selectivity. In contrast, substituting it with bulkier amino acids such as phenylalanine, tyrosine, tryptophan, or even smaller cysteine resulted in decreased *S*-selectivity (Figure 4D). The residue G248 proved critical for enhancing *S*-selectivity, with mutations to bulkier amino acids consistently leading to significant improvements. The enhancement in selectivity by mutations at G248 was not previously reported, likely because past analytical strategies did not simultaneously screen for conversion and enantioselectivity. To further improve the enantioselectivity of the enzyme, we conducted additional rounds of screening using iterative saturation mutagenesis (ISM).^{62,63} Following iterative optimization, the final mutant, IRED-195-R2, was able to synthesize the target intermediate with 99% ee (*S*) and 72% yield on a 2.5 mmol scale (Table S9 in the SI). Collectively, our approach enables us to elucidate the relationship between enzyme activity, selectivity, and individual residues with greater precision. The robust enhancement in selectivity underscores the efficacy of our high-throughput screening platform for directed evolution.

CONCLUSIONS

In summary, we have developed a novel ¹⁹F NMR-based high-throughput platform for screening imine reductases. This approach outperforms traditional chiral chromatographic analysis, achieving a more than 10-fold improvement in time efficiency for enantioanalysis. It allows for the simultaneous determination of yields and enantioselectivity, providing a more comprehensive data set compared to methods that only measure conversion or enantioselectivity. Capable of screening over 1,000 biosynthetic reactions, this platform is well-suited for use in directed evolution processes. Previous directed evolution workflows typically prioritize initial screening for catalytic activity, with enantioselectivity assessed only in subsequent stages. In contrast, by simultaneously monitoring both conversion and enantioselectivity, our method not only identifies variants with improved activity and selectivity but also captures mutants that exhibit enhanced stereocontrol despite reduced activity. This integrated approach enables a more nuanced and comprehensive strategy for biocatalyst engineering, where even "suboptimal" variants provide valuable mechanistic insights that can inform the rational design of enzymes balancing both activity and stereochemical precision. Moreover, its application extends beyond imine reductases to include other enzymatic reactions, such as those involving chiral alcohols, nitriles, and sulfoxides, contingent upon the use of a ¹⁹F-labeled probe with appropriate recognition properties. The ability to generate distinct ¹⁹F NMR signals for each enantiomer ensures excellent compatibility with complex matrices. This capability paves the way for the screening of more intricate biological processes and establishes the platform as a robust tool for advancing enzyme engineering and biocatalysis research.

ASSOCIATED CONTENT

Supporting Information

The Supporting Information is available free of charge at <https://pubs.acs.org/doi/10.1021/acscentsci.5c00498>.

General information about materials and instruments, procedures for NMR experiments, NMR spectra, HPLC traces; details of analytical protocols and bioinformatics data ([PDF](#))

AUTHOR INFORMATION

Corresponding Authors

Liang Lin – State Key Laboratory of Chemical Biology, Shanghai Institute of Organic Chemistry, University of Chinese Academy of Sciences, Shanghai 200032, China; Email: lianglin@mail.sioc.ac.cn

Yanchuan Zhao – State Key Laboratory of Fluorine and Nitrogen Chemistry and Advanced Materials and Shanghai Hongkong Joint Laboratory in Chemical Synthesis, Shanghai Institute of Organic Chemistry, University of Chinese Academy of Sciences, Chinese Academy of Sciences, Shanghai 200032, China; Instrumental Analysis Center, Shanghai Institute of Organic Chemistry, Chinese Academy of Sciences, Shanghai 200032, China; orcid.org/0000-0002-2903-4218; Email: zhaoyanchuan@sioc.ac.cn

Authors

Shucheng Song – State Key Laboratory of Chemical Biology, Shanghai Institute of Organic Chemistry, University of Chinese Academy of Sciences, Shanghai 200032, China

Chenyang Wang – State Key Laboratory of Fluorine and Nitrogen Chemistry and Advanced Materials and Shanghai Hongkong Joint Laboratory in Chemical Synthesis, Shanghai Institute of Organic Chemistry, University of Chinese Academy of Sciences, Chinese Academy of Sciences, Shanghai 200032, China

Wenjing Bao – State Key Laboratory of Fluorine and Nitrogen Chemistry and Advanced Materials and Shanghai Hongkong Joint Laboratory in Chemical Synthesis, Shanghai Institute of Organic Chemistry, University of Chinese Academy of Sciences, Chinese Academy of Sciences, Shanghai 200032, China

Zhenchuang Xu – State Key Laboratory of Fluorine and Nitrogen Chemistry and Advanced Materials and Shanghai Hongkong Joint Laboratory in Chemical Synthesis, Shanghai Institute of Organic Chemistry, University of Chinese Academy of Sciences, Chinese Academy of Sciences, Shanghai 200032, China

Jian Wu – Instrumental Analysis Center, Shanghai Institute of Organic Chemistry, Chinese Academy of Sciences, Shanghai 200032, China

Complete contact information is available at:

<https://pubs.acs.org/10.1021/acscentsci.5c00498>

Author Contributions

¹S.S. and C.W. contributed equally.

Notes

The authors declare no competing financial interest.

ACKNOWLEDGMENTS

This study was supported by the Natural Science Foundation of China (22271305) and National Key Research and Development (R&D) Program Project (2022YFA1505600),

the Strategic Priority Research Program of the Chinese Academy of Sciences (XDB0590000), and the International Partnership Program of Chinese Academy of Sciences for future network (033GJHZ2022055FN). Y.Z. thanks Byungjin Koo for helpful discussion.

ABBREVIATIONS

WT,wild type; IRED,imine reductase; BLAST,Basic Local Alignment Search Tool; NCBI,National Center for Biotechnology information.

REFERENCES

- (1) Wu, S.; Snajdrova, R.; Moore, J. C.; Baldenius, K.; Bornscheuer, U. T. Biocatalysis: Enzymatic Synthesis for Industrial Applications. *Angew. Chem., Int. Ed.* **2021**, *60*, 88–119.
- (2) Bornscheuer, U. T.; Huisman, G. W.; Kazlauskas, R. J.; Lutz, S.; Moore, J. C.; Robins, K. Engineering the third wave of biocatalysis. *Nature* **2012**, *485*, 185–194.
- (3) Sheldon, R. A.; Woodley, J. M. Role of Biocatalysis in Sustainable Chemistry. *Chem. Rev.* **2018**, *118*, 801–838.
- (4) Clouthier, C. M.; Pelletier, J. N. Expanding the organic toolbox: a guide to integrating biocatalysis in synthesis. *Chem. Soc. Rev.* **2012**, *41*, 1585–1605.
- (5) Ran, N.; Zhao, L.; Chen, Z.; Tao, J. Recent applications of biocatalysis in developing green chemistry for chemical synthesis at the industrial scale. *Green Chem.* **2008**, *10*, 361–372.
- (6) Winkler, C. K.; Schrittwieser, J. H.; Kroutil, W. Power of Biocatalysis for Organic Synthesis. *ACS Cent. Sci.* **2021**, *7*, 55–71.
- (7) Christianson, D. W. Structural and Chemical Biology of Terpenoid Cyclases. *Chem. Rev.* **2017**, *117*, 11570–11648.
- (8) Auclair, K.; Sutherland, A.; Kennedy, J.; Witter, D. J.; Van den Heever, J. P.; Hutchinson, C. R.; Vederas, J. C. Lovastatin Nonaketide Synthase Catalyzes an Intramolecular Diels–Alder Reaction of a Substrate Analogue. *J. Am. Chem. Soc.* **2000**, *122*, 11519–11520.
- (9) Ose, T.; Watanabe, K.; Mie, T.; Honma, M.; Watanabe, H.; Yao, M.; Oikawa, H.; Tanaka, I. Insight into a natural Diels–Alder reaction from the structure of macrophomate synthase. *Nature* **2003**, *422*, 185–189.
- (10) Kim, H. J.; Ruszczycky, M. W.; Choi, S.-h.; Liu, Y.-n.; Liu, H.-w. Enzyme-catalysed [4 + 2] cycloaddition is a key step in the biosynthesis of spinosyn A. *Nature* **2011**, *473*, 109–112.
- (11) Wang, H.; Zou, Y.; Li, M.; Tang, Z.; Wang, J.; Tian, Z.; Strassner, N.; Yang, Q.; Zheng, Q.; Guo, Y.; Liu, W.; Pan, L.; Houk, K. N. A cyclase that catalyses competing 2 + 2 and 4 + 2 cycloadditions. *Nat. Chem.* **2023**, *15*, 177–184.
- (12) Zhang, X.; King-Smith, E.; Renata, H. Total Synthesis of Tambromycin by Combining Chemocatalytic and Biocatalytic C–H Functionalization. *Angew. Chem., Int. Ed.* **2018**, *57*, 5037–5041.
- (13) Lazzarotto, M.; Hammerer, L.; Hetmann, M.; Borg, A.; Schmermund, L.; Steiner, L.; Hartmann, P.; Belaj, F.; Kroutil, W.; Gruber, K.; Fuchs, M. Chemoenzymatic Total Synthesis of Deoxy-, epi-, and Podophyllotoxin and a Biocatalytic Kinetic Resolution of Dibenzylbutyrolactones. *Angew. Chem., Int. Ed.* **2019**, *58*, 8226–8230.
- (14) Ortiz de Montellano, P. R. Hydrocarbon Hydroxylation by Cytochrome P450 Enzymes. *Chem. Rev.* **2010**, *110*, 932–948.
- (15) Stout, C. N.; Renata, H. Reinvigorating the Chiral Pool: Chemoenzymatic Approaches to Complex Peptides and Terpenoids. *Acc. Chem. Res.* **2021**, *54*, 1143–1156.
- (16) Zwick, C. R., III; Renata, H. Remote C–H Hydroxylation by an α -Ketoglutarate-Dependent Dioxygenase Enables Efficient Chemoenzymatic Synthesis of Manzacidin C and Proline Analogs. *J. Am. Chem. Soc.* **2018**, *140*, 1165–1169.
- (17) Chakrabarty, S.; Wang, Y.; Perkins, J. C.; Narayan, A. R. H. Scalable biocatalytic C–H oxyfunctionalization reactions. *Chem. Soc. Rev.* **2020**, *49*, 8137–8155.
- (18) Xiao, H.; Bao, Z.; Zhao, H. High Throughput Screening and Selection Methods for Directed Enzyme Evolution. *Ind. Eng. Chem. Res.* **2015**, *54*, 4011–4020.

- (19) Wang, T.-C.; Mai, B. K.; Zhang, Z.; Bo, Z.; Li, J.; Liu, P.; Yang, Y. Stereoselective amino acid synthesis by photobiocatalytic oxidative coupling. *Nature* **2024**, *629*, 98–104.
- (20) Cheng, L.; Li, D.; Mai, B. K.; Bo, Z.; Cheng, L.; Liu, P.; Yang, Y. Stereoselective amino acid synthesis by synergistic photoredox-pyridoxal radical biocatalysis. *Science* **2023**, *381*, 444–451.
- (21) Li, M.; Yuan, Y.; Harrison, W.; Zhang, Z.; Zhao, H. Asymmetric photoenzymatic incorporation of fluorinated motifs into olefins. *Science* **2024**, *385*, 416–421.
- (22) Harrison, W.; Jiang, G.; Zhang, Z.; Li, M.; Chen, H.; Zhao, H. Photoenzymatic Asymmetric Hydroamination for Chiral Alkyl Amine Synthesis. *J. Am. Chem. Soc.* **2024**, *146*, 10716–10722.
- (23) Xing, Z.; Liu, F.; Feng, J.; Yu, L.; Wu, Z.; Zhao, B.; Chen, B.; Ping, H.; Xu, Y.; Liu, A.; Zhao, Y.; Wang, C.; Wang, B.; Huang, X. Synergistic photobiocatalysis for enantioselective triple-radical sorting. *Nature* **2025**, *637*, 1118–1123.
- (24) Xu, Y.; Chen, H.; Yu, L.; Peng, X.; Zhang, J.; Xing, Z.; Bao, Y.; Liu, A.; Zhao, Y.; Tian, C.; Liang, Y.; Huang, X. A light-driven enzymatic enantioselective radical acylation. *Nature* **2024**, *625*, 74–78.
- (25) Biegasiewicz, K. F.; Cooper, S. J.; Gao, X.; Oblinsky, D. G.; Kim, J. H.; Garfinkle, S. E.; Joyce, L. A.; Sandoval, B. A.; Scholes, G. D.; Hyster, T. K. Photoexcitation of flavoenzymes enables a stereoselective radical cyclization. *Science* **2019**, *364*, 1166–1169.
- (26) Reetz, M. T.; Becker, M. H.; Klein, H.-W.; Stöckigt, D. A Method for High-Throughput Screening of Enantioselective Catalysts. *Angew. Chem., Int. Ed.* **1999**, *38*, 1758–1761.
- (27) Reetz, M. T.; Eipper, A.; Tielmann, P.; Mynott, R. A Practical NMR-Based High-Throughput Assay for Screening Enantioselective Catalysts and Biocatalysts. *Adv. Synth. Catal.* **2002**, *344*, 1008–1016.
- (28) Reetz, M. T.; Becker, M. H.; Kühling, K. M.; Holzwarth, A. Time-Resolved IR-Thermographic Detection and Screening of Enantioselectivity in Catalytic Reactions. *Angew. Chem., Int. Ed.* **1998**, *37*, 2647–2650.
- (29) Janes, L. E.; Kazlauskas, R. J. QuickE. A Fast Spectrophotometric Method To Measure the Enantioselectivity of Hydrolases. *J. Org. Chem.* **1997**, *62*, 4560–4561.
- (30) Swoboda, A.; Pfeifenberger, L. J.; Duhović, Z.; Bürgler, M.; Oroz-Guinea, I.; Bangert, K.; Weißensteiner, F.; Parigger, L.; Ebner, K.; Glieder, A.; Kroutil, W. Enantioselective High-Throughput Assay Showcased for the Identification of (R)- as well as (S)-Selective Unspecific Peroxygenases for C–H Oxidation. *Angew. Chem., Int. Ed.* **2023**, *62*, No. e202312721.
- (31) Leung, D.; Kang, S. O.; Anslyn, E. V. Rapid determination of enantiomeric excess: a focus on optical approaches. *Chem. Soc. Rev.* **2012**, *41*, 448–479.
- (32) Jo, H. H.; Lin, C.-Y.; Anslyn, E. V. Rapid Optical Methods for Enantiomeric Excess Analysis: From Enantioselective Indicator Displacement Assays to Exciton-Coupled Circular Dichroism. *Acc. Chem. Res.* **2014**, *47*, 2212–2221.
- (33) Wolf, C.; Bentley, K. W. Chirality sensing using stereodynamic probes with distinct electronic circular dichroism output. *Chem. Soc. Rev.* **2013**, *42*, 5408–5424.
- (34) Bentley, K. W.; Zhang, P.; Wolf, C. Miniature high-throughput chemosensing of yield, ee, and absolute configuration from crude reaction mixtures. *Sci. Adv.* **2016**, *2*, No. e1501162.
- (35) Hirose, K.; Fujiwara, A.; Matsunaga, K.; Aoki, N.; Tobe, Y. Chiral recognition of secondary amines by using chiral crown ether and podand. *Tetrahedron Lett.* **2002**, *43*, 8539–8542.
- (36) Jiang, L.; Tian, J.; Zhao, F.; Yu, S.; Shi, D.; Wang, X.; Yu, X.; Pu, L. Fluorescent Recognition of Functional Secondary Amines in the Fluorous Phase. *Eur. J. Org. Chem.* **2019**, *2019*, 2533–2538.
- (37) Gu, G.; Zhao, C.; Zhang, W.; Weng, J.; Xu, Z.; Wu, J.; Xie, Y.; He, X.; Zhao, Y. Chiral Discrimination of Acyclic Secondary Amines by ¹⁹F NMR. *Anal. Chem.* **2024**, *96*, 730–736.
- (38) Xu, Z.; Liu, C.; Zhao, S.; Chen, S.; Zhao, Y. Molecular Sensors for NMR-Based Detection. *Chem. Rev.* **2019**, *119*, 195–230.
- (39) Li, Y.; Wen, L.; Meng, H.; Lv, J.; Luo, G.; Zhao, Y. Separation-free Enantiodifferentiation with Chromatogram-like Output. *Cell Rep. Phys. Sci.* **2020**, *1*, 100100.
- (40) Xu, Z.; Wang, C.; He, S.; Wu, J.; Zhao, Y. Enhancing Molecular-Level Biological Monitoring with a Smart Self-Assembling ¹⁹F-Labeled Probe. *Angew. Chem., Int. Ed.* **2025**, *64*, No. e202417112.
- (41) Chen, Y.-T.; Li, B.; Chen, J.-L.; Su, X.-C. Simultaneous Discrimination and Quantification of Enantiomeric Amino Acids under Physiological Conditions by Chiral ¹⁹F NMR Tag. *Anal. Chem.* **2022**, *94*, 7853–7860.
- (42) Wang, W.; Xia, X.; Bian, G.; Song, L. A Chiral Sensor for Recognition of Varied Amines Based on ¹⁹F NMR Signals of Newly Designed Rhodium Complexes. *Chem. Commun.* **2019**, *55*, 6098–6101.
- (43) Duong, Q.; Kwahk, E.-J.; Kim, J.; Park, H.; Cho, H.; Kim, H. Bioinspired Fluorine Labeling for ¹⁹F NMR-Based Plasma Amine Profiling. *Anal. Chem.* **2024**, *96*, 1614–1621.
- (44) Gu, G.; Xu, Z.; Wen, L.; Liang, J.; Wang, C.; Wan, X.; Zhao, Y. Chirality Sensing of N-Heterocycles via ¹⁹F NMR. *JACS Au* **2023**, *3*, 1348–1357.
- (45) France, S. P.; Howard, R. M.; Steflik, J.; Weise, N. J.; Mangas-Sánchez, J.; Montgomery, S. L.; Crook, R.; Kumar, R.; Turner, N. J. Identification of Novel Bacterial Members of the Imine Reductase Enzyme Family that Perform Reductive Amination. *ChemCatChem.* **2018**, *10*, 510–514.
- (46) Zhan, Z. Z.; Xu, Z. F.; Yu, S. S.; Feng, J. H.; Liu, F. F.; Yao, P. Y.; Wu, Q. Q.; Zhu, D. M. Stereocomplementary Synthesis of a Key Intermediate for Tofacitinib via Enzymatic Dynamic Kinetic Resolution-Reductive Amination. *Adv. Synth. Catal.* **2022**, *364*, 2380–2386.
- (47) Aleku, G. A.; France, S. P.; Man, H.; Mangas-Sánchez, J.; Montgomery, S. L.; Sharma, M.; Leipold, F.; Hussain, S.; Grogan, G.; Turner, N. J. A reductive aminase from *Aspergillus oryzae*. *Nat. Chem.* **2017**, *9*, 961–969.
- (48) Kumar, R.; Karmilowicz, M. J.; Burke, D.; Burns, M.; Clark, L. A.; Connor, C. G.; Cordi, E.; Do, N. M.; Doyle, K. M.; Hoagland, S.; Lewis, C. A.; Mangan, D.; Martinez, C. A.; McInturff, E. L.; Meldrum, K.; Pearson, R.; Steflik, J.; Rane, A.; Weaver, J. Biocatalytic reductive amination from discovery to commercial manufacturing applied to abrocitinib JAK1 inhibitor. *Nat. Catal.* **2021**, *4*, 775–782.
- (49) Thorpe, T. W.; Marshall, J. R.; Harawa, V.; Ruscoe, R. E.; Cuetos, A.; Finnigan, J. D.; Angelastro, A.; Heath, R. S.; Parmeggiani, F.; Charnock, S. J.; Howard, R. M.; Kumar, R.; Daniels, D. S. B.; Grogan, G.; Turner, N. J. Multifunctional biocatalyst for conjugate reduction and reductive amination. *Nature* **2022**, *604*, 86–91.
- (50) Roiban, G.-D.; Kern, M.; Liu, Z.; Hyslop, J.; Tey, P. L.; Levine, M. S.; Jordan, L. S.; Brown, K. K.; Hadi, T.; Ihnken, L. A. F.; Brown, M. J. B. Efficient Biocatalytic Reductive Aminations by Extending the Imine Reductase Toolbox. *ChemCatChem.* **2017**, *9*, 4475–4479.
- (51) Ma, E. J.; Siiriola, E.; Moore, C.; Kummer, A.; Stoeckli, M.; Faller, M.; Bouquet, C.; Eggimann, F.; Ligibel, M.; Huynh, D.; Cutler, G.; Siegrist, L.; Lewis, R. A.; Acker, A. C.; Freund, E.; Koch, E.; Vogel, M.; Schlingensiepen, H.; Oakeley, E. J.; Snajdrova, R. Machine-Directed Evolution of an Imine Reductase for Activity and Stereoselectivity. *ACS Catal.* **2021**, *11*, 12433–12445.
- (52) Xu, Z.; Yao, P.; Sheng, X.; Li, J.; Li, J.; Yu, S.; Feng, J.; Wu, Q.; Zhu, D. Biocatalytic Access to 1,4-Diazepanes via Imine Reductase-Catalyzed Intramolecular Asymmetric Reductive Amination. *ACS Catal.* **2020**, *10*, 8780–8787.
- (53) Zhu, J. M.; Tan, H. Q.; Yang, L.; Dai, Z.; Zhu, L.; Ma, H. M.; Deng, Z. X.; Tian, Z. H.; Qu, X. D. Enantioselective Synthesis of 1-Aryl-Substituted Tetrahydroisoquinolines Employing Imine Reductase. *ACS Catal.* **2017**, *7*, 7003–7007.
- (54) Li, H.; Luan, Z. J.; Zheng, G. W.; Xu, J. H. Efficient Synthesis of Chiral Indolines using an Imine Reductase from *Paenibacillus lacticis*. *Adv. Synth. Catal.* **2015**, *357*, 1692–1696.
- (55) Leipold, F.; Hussain, S.; Ghislieri, D.; Turner, N. J. Asymmetric Reduction of Cyclic Imines Catalyzed by a Whole-Cell Biocatalyst

Containing an (S)-Imine Reductase. *ChemCatChem.* **2013**, *5*, 3505–3508.

(56) Zhang, J.; Liao, D. H.; Chen, R. C.; Zhu, F. F.; Ma, Y. Q.; Gao, L.; Qu, G.; Cui, C. S.; Sun, Z. T.; Lei, X. G.; Gao, S. S. Tuning an Imine Reductase for the Asymmetric Synthesis of Azacycloalkylamines by Concise Structure-Guided Engineering. *Angew. Chem., Int. Ed.* **2022**, *61*, No. e202201908.

(57) Schober, M.; MacDermaid, C.; Ollis, A. A.; Chang, S.; Khan, D.; Hosford, J.; Latham, J.; Ihnken, L. A. F.; Brown, M. J. B.; Fuerst, D.; Sanganee, M. J.; Roiban, G. D. Chiral synthesis of LSD1 inhibitor GSK2879552 enabled by directed evolution of an imine reductase. *Nat. Catal.* **2019**, *2*, 909–915.

(58) Wang, Z.; Gao, G. S.; Gao, Y. D.; Yang, L. C. Application of Imine Reductase in Bioactive Chiral Amine Synthesis. *Org. Process Res. Dev.* **2024**, *28*, 3035–3054.

(59) Aleku, G. A. Imine Reductases and Reductive Aminases in Organic Synthesis. *ACS Catal.* **2024**, *14*, 14308–14329.

(60) Citoler, J.; Harawa, V.; Marshall, J. R.; Bevinakatti, H.; Finnigan, J. D.; Charnock, S. J.; Turner, N. J. Synthesis of Pharmaceutically Relevant 2-Aminotetralin and 3-Aminochroman Derivatives via Enzymatic Reductive Amination. *Angew. Chem., Int. Ed.* **2021**, *60*, 24456–24460.

(61) Tang, D. Y.; Ma, Y. Q.; Bao, J. P.; Gao, S. S.; Man, S. L.; Cui, C. S. Chemoenzymatic total synthesis of rotigotine *via* IRED-catalyzed reductive amination. *Org. Biomol. Chem.* **2024**, *22*, 3843–3847.

(62) Reetz, M. T.; Wang, L.-W.; Bocola, M. Directed Evolution of Enantioselective Enzymes: Iterative Cycles of CASTing for Probing Protein-Sequence Space. *Angew. Chem., Int. Ed.* **2006**, *45*, 1236–1241.

(63) Reetz, M. T.; Carballeira, J. D. Iterative saturation mutagenesis (ISM) for rapid directed evolution of functional enzymes. *Nat. Protoc.* **2007**, *2*, 891–903.